Research Square

Preprints are preliminary reports that have not undergone peer review.
They should not be considered conclusive, used to inform clinical practice,
or referenced by the media as validated information.

Measuring Coherent Radio and Microwave Photons from the Solar Corona

Liang Chen
Chizhou University
Zizang Qiu
Zizang.Qiu@ed.ac.uk

University of Edinburgh
Tom Kephart
Vanderbilt University
Arjun Berera
University of Edinburgh

Research Article

Keywords: Corona, Radio Emission, Theory, Spectral Line, Plasma Physics

Posted Date: March 27th, 2026

DOI: https://doi.org/10.21203/rs.3.rs-8887271/v1

License: This work is licensed under a Creative Commons Attribution 4.0 International License.
Read Full License

Additional Declarations: No competing interests reported.

Measuring Coherent Radio and Microwave Photons from the Solar Corona

Liang Chen[1] · **Zizang Qiu**[2] · **Tom Kephart**[3] · **Arjun Berera**[2]

© **The author(s)** ●●●●

Abstract The rates of production of radio/microwave N-identical photons states $|N\rangle$ from stimulated emission in the solar atmosphere are estimated. Effects of various decohering factors are shown to be small. Ground based measurements of these quantum states via the inverse Hong-Ou-Mandel effect are proposed. We argue that a signal is detectable and far above the noise in several cases.

Keywords: Corona, Radio Emission, Theory, Spectral Line, Plasma Physics

1. Introduction

Photons in certain frequency bands can sustain quantum coherence at interstellar distances (Berera 2020), which introduces quantum mechanical interests into astronomical observation. By quantum coherence we mean N photons in some specified quantum state, which particularly in this paper means they are all identical, with the same momentum and polarization. On a much longer scale, quantum coherence at cosmological distances can also be preserved as decoherence effects from interactions with the cosmological medium and the expansion

✉ L. Chen
bqipd@pm.me

✉ Z. Qiu
zizang.qiu@ed.ac.uk

✉ T. Kephart
tom.kephart@gmail.com

✉ A. Berera
ab@ed.ac.uk

[1] Research Center of Applied Physics and Photoelectric Information, Chizhou University, Chizhou, Anhui, 247000, China

[2] School of Physics and Astronomy, University of Edinburgh, Edinburgh, EH9 3FD, United Kingdom

[3] Department of Physics and Astronomy, Vanderbilt University, Nashville, TN 37235, USA

of the Universe are negligible (Berera et al. 2021). Viability of using photons in X-ray, optical and microwave bands as candidates to establish interstellar quantum communications was studied in Berera and Calderón-Figueroa (2022) and more recently in Boyle (2024).

In Berera et al. (2023) a novel observation was made by us that stimulated emission(SE) processes can occur in the solar atmosphere and in some regimes can propagate through the solar atmosphere and solar system without decohering, and so could be measurable near Earth. This stimulated emission process of N identical photons produced in a specified quantum state, which we denote as $|N\rangle$, is a possible type of astrophysically sourced quantum coherent photonic signal. Such signals deep below the surface of the Sun or star would quickly decohere through interactions. But SE in the stellar atmosphere could still yield surviving coherent signals with the quantum nature intact. We proposed this possibility and did some initial estimates of the rates of potentially detectable $|2\rangle$ states on a 1 m^2 area near Earth from SE occurring in the Solar corona, for characteristic optical, UV and X-ray emission lines (Berera et al. 2023). These optical/UV/X-ray $|2\rangle$ rates are low and rates for $|N\rangle$ with $N \geq 3$ are near 0, but it can be worth exploring the rates of $|2\rangle$ states at other frequencies such as radio and microwave, which will be strong candidates for experimental verification if the estimated rates are high.

The main focus of this paper is at the source end of the process in obtaining more detailed estimates than those in Berera et al. (2023) of SE events created in the solar atmosphere. We also give some further guidelines related to the receiving end, in regards the type of experiment that could detect such events, though we are not attempting a detailed examination of that at this stage. In this respect, the basic experiment to test for the SE pairs we suggest is based on the Hong-Ou-Mandel(HOM) effect (Hong, Ou, and Mandel 1987). Quantum interferences based on the HOM effect have already been conducted between solar photons and quantum dot photons (Deng et al. 2019). The measurement we propose in this paper is qualitatively distinct from Deng et al. (2019) in that our work focuses on the detection of photon multiplets $|N\rangle$ produced directly from stimulated emission via self-interference, in contrast to the interference of two photon singlets discussed in Deng et al. (2019) and Duan et al. (2020). Thus, although the measurement methodology of our work will be similar to that used by Deng et al. (2019) and Duan et al. (2020), the underlying physics being tested is very different. The physics here is based on quantum coherence created entirely within an astrophysical body, i.e., the stimulated emission photons created in the solar corona, whereas the above mentioned work (Deng et al. 2019; Duan et al. 2020) are testing something different as their photons from the Sun are simply singlet states. Another difference with our work, developing out of our past analysis (Berera 2020; Berera et al. 2021; Berera and Calderón-Figueroa 2022; Berera et al. 2023), is that we continue our extensive study to identify decohering background effects in the Solar and interplanetary medium, that could potentially destroy or distort the signal. The experiments in Deng et al. (2019) and Duan et al. (2020) were very specific and did not need tests for background decoherence effects. However, for general tests searching for quantum coherence from astrophysical sources, decoherence from background effects is a concern

that needs to be addressed. Note that the HOM effect differs fundamentally from the Hanburry-Brown-Twiss (HBT) effect (BROWN and TWISS 1956). While a semiclassical approach can fully account for the HBT effect, the HOM effect requires a quantum mechanical treatment to be accurately described.

Valuable discussions of the mechanism of SE can be found in Townsend (2012); Svelto (2010). According to Fermi's Golden Rule, a Bose enhancement factor arises for the transition probability amplitude of stimulated photon emission, leading to a higher chance of obtaining states with a large number of photons of the same momentum and polarization. In Berera et al. (2023), we re-expressed the cross section of SE in terms of the wavelength λ_0, refraction index n of the material, wavelength width of the emission $\Delta\lambda$, and rate of spontaneous emission A, as

$$\sigma_0 = \left(\frac{\lambda_0}{2\pi n}\right)^2 \left(\frac{A\lambda_0}{c}\right) \left(\frac{\lambda_0}{\Delta\lambda}\right) \ . \tag{1}$$

Using NIST data (Kramida et al. 2023) for the numerical values of A allows us to calculate cross sections of any SE line from any atom or ion.

In real scenarios, all photons are accompanied by some level of broadening. The cross-section of SE depends on the linewidth; therefore, even if there is a wavelength mismatch, SE can still occur, but with a lower probability and consequently a reduced chance for Bose enhancement.

A single photon state $|1\rangle$ traveling through a layer of type a excited atoms with number density n_a can become a multi-photon state $|N\rangle$ after a distance x due to SE. Here the distance x is not used to localize the photon but only to label the location where measurements may be performed. Denoting the probability of finding an $|N\rangle$ state by $P(x, N)$, Berera et al. (2023) shows that

$$P(x, N) = e^{-n_a \sigma_0 x} \left(1 - e^{-n_a \sigma_0 x}\right)^{N-1} \ . \tag{2}$$

$P(x, N)$ is normalized to 1, when summed over all N, independent of x.

This resembles a phenomenological rate equation that describes the growth of multiplets of condensed states.

We have done an extensive search of possible SE processes in the solar atmosphere. In this Letter we report identification of a process in the microwave region that we will show produces a sizable rate and at the same time is amenable to measurement by a ground based experiment on Earth. The Letter starts by first providing a broader range of SE processes, giving estimates for how uncertainties are treated. Next we identify potential sources of decoherence and show that these are not significant. We then discuss the uncertainties involved and compare the rates for the microwave to radio band to those of Optical, UV, X-ray given in Berera et al. (2023). We also propose how measurements could be performed to detect these quantum states via the time reversed HOM test, focusing in particular on the microwave range, which is the key case of interest in this paper.

2. Rate Estimations

We estimate the rate of $|1\rangle$-states produced by the Sun based on the measured values of the photon fluxes for various frequencies. As these $|1\rangle$ states travel through the solar corona, they can stimulate a layer of excited atoms and become $|2\rangle$ or $|3\rangle$ states and so forth. We then determine the rate of these $|N\rangle$ states detectable on a 1 m^2 area near the Earth.

We shall first consider photons in the radio to microwave regions. Thousands of solar radio bursts occurring on different dates in the frequency range of 100-500 MHz observed by Ikarus/Zurich were analyzed (Aschwanden, Benz, and Montello 1994). In this frequency range, we select 117 MHz to investigate since it is a transition line between two energy levels of hydrogen. The minimum solar flux between 105 and 120 MHz was measured to be around 140 solar flux units (SFU) Aschwanden, Benz, and Montello (1994), which is equal to 1.4×10^{-20} W/(m^2·Hz) and translates to an energy flux of 2.1×10^{-13} W/m^2.

The ratio $\Delta\lambda/\lambda_0 = 0.1\%$ is a reasonable estimate (Svelto 2010) to use in eq.(1) to account for the SE linewidth. This implies an energy flux of 1.5×10^{-15} W/m^2 and a photon number flux of 1.94×10^{10} s^{-1} m^{-2} at 117 MHz. Thus we take the rate of $|1\rangle$ state as $N_1(117\text{ MHz}) \sim 1.94 \times 10^{10}$.

The 117 MHz comes from transition between two energy levels of neutral hydrogen. But hydrogen will be ionized in deep corona regions because of the high temperature. Therefore, SE could only occur across a thin layer just above the photosphere. The thickness of the layer is about $L = 2 \times 10^6$ m according to the electron density and temperature model of the chromosphere (Fontenla, Avrett, and Loeser 1990; Gabriel 1976). We can think of the hydrogen atoms in this layer as being in thermal equilibrium since they are at the boundary of the photosphere. However, only those neutral hydrogen atoms that are in the upper level of the 117 MHz line are able to be stimulated by the 117 MHz photons. After calculating the Boltzmann factors of all the energy levels of a hydrogen atom listed by NISTKramida et al. (2023) at temperature $T = 5800$ K, the fraction of these stimulable hydrogen atoms is given by

$$\frac{e^{-E_0/k_BT}}{\sum_i e^{-E_i/k_BT}} \sim 4.53 \times 10^{-12} \ , \tag{3}$$

where E_0 is the energy of the stimulable hydrogen atoms, E_i are the energies of hydrogen atoms at various energy levels and k_B is the Boltzmann constant. For the density of hydrogen atoms, we take the modest estimate of 10^{18} m^{-3}, though even higher number densities are suggested, depending on the height above the photosphere (Fontenla, Avrett, and Loeser 1990; Gabriel 1976). Thus the density of stimulable hydrogen atoms is roughly $n_{\rm H} = 4.5 \times 10^6$ m^{-3}.

Substituting the rate $A = 4.6551 \times 10^{-11}$ s^{-1} Kramida et al. (2023) of spontaneous emission of a 117 MHz photon from a hydrogen atom on the corresponding energy level into eq.(1), results in a cross section $\sigma_0 = 6.6 \times 10^{-17}$ m^2 for SE. Given the density of hydrogen atoms and the cross section, the mean free path (MFP) of the SE is calculated to be about 3.34×10^9 m.

Following the path of a $|1\rangle$ state, the probability of finding a $|2\rangle$ state at a distance L is $P(L, 2)$. Since we have estimated the rate of $|1\rangle$-states $N_1(117\text{ MHz})$

in the discussion above, the rate of detectable $|2\rangle$-states $N_2(117\text{ MHz})$ can be computed by applying eq. (2),

$$\begin{aligned} N_2(117\text{ MHz}) =& N_1(117\text{ MHz}) \times e^{-n_{\rm H}\sigma_0 L}\left(1 - e^{-n_{\rm H}\sigma_0 L}\right) \\ \approx& 1.16 \times 10^7 \text{ per s} . \end{aligned}$$

This means that among all the 117 MHz photons impinging upon an area of 1 m^2 near Earth in one hour, there are over 11 million $|2\rangle$ states.

Besides the 117 MHz band in the radio, we also find the rate of $|1\rangle$-states for 232 MHz based on the time profile of radio flux from the Ikarus/Zurich observations Aschwanden et al. (1995). While in the microwave range, we gather the data of $|1\rangle$-state rates for 1.078 GHz, 1.2378 GHz, 1.3711 GHz, 2.9334 GHz, 3.245 GHz and 9.9112 GHz respectively, from a spectral fit of the analysis of solar flares detected by the Owens Valley Solar Array(OVSA)Nita, Gary, and Lee (2004). These frequencies are in the radio to microwave range that could come from SE of hydrogen atoms Kramida et al. (2023). We did not find relevant rates of SE in this range from other atoms/ions. Following similar procedures laid out above, we present the calculated rates $N_2(\nu_0)$ of $|2\rangle$-state for these frequencies ν_0 in table 2 below. Across the spectrum, among the photons impinging upon an

Table 1. Estimates of the rates of $|2\rangle$-state, $|3\rangle$-state and $|4\rangle$-state in the radio and microwave range.

ν_0 (GHz)	$N_1(\nu_0)$ s^{-1}	$N_2(\nu_0)$ s^{-1}	$N_3(\nu_0)$ s^{-1}	$N_4(\nu_0)$ s^{-1}
0.117	1.94×10^{10}	1.16×10^7	6953	4.16
0.232	1.20×10^{10}	8.40×10^6	6093	4.41
1.078	1.30×10^{11}	8.17×10^6	514	0.03
1.2378	9.85×10^{10}	4.28×10^7	18688	8.14
1.3711	8.03×10^{10}	9.31×10^6	1081	0.12
2.9334	1.75×10^{10}	7.63×10^6	3327	1.44
3.245	1.43×10^{10}	6.24×10^6	2719	1.18
9.9112	1.54×10^{9}	2.87×10^7	547938	10447

area of 1 m^2 near Earth in per second, millions of $|2\rangle$-states, and from hundreds to half a million $|3\rangle$-states could be measurable, depending on the efficiency of the instruments. Even if the original measurements were performed by different research teams with different equipment at different locations and times, values of $N_2(\nu_0)$ in table 2 are of similar order of magnitudes.

Note that the hydrogen density varies by more than 9 orders of magnitude in different parts of the solar atmosphere (for instance, the lowest particle density found in corona holes is 5×10^9 m^{-3} (Morgan and Cook 2020)). Thus it should be noted that the lower value of this density then gives a cautious estimate for SE rates which could be reduced by orders of magnitude comparing to those found in table 2.

Note that differences between values of $|3\rangle$-state rates $N_3(\nu_0)$ in table 2 diverge, and the values of $|4\rangle$-state rates $N_4(\nu_0)$ diverge further, varying from

3×10^{-2} to 1×10^{4}. This divergence occurs as a manifestation of different MFPs for photons of different frequencies. For example, the MFPs for photons of 1.078 GHz and 9.9112 GHz are around 3.17×10^{10} m and 1.04×10^{8} m, respectively. To create a $|4\rangle$-state from a $|1\rangle$-state, there needs to be three consecutive events of SE. The two orders of magnitude difference in MFPs gets cubed when calculating these rates, resulting in roughly six orders of magnitude difference between N_4(1.078 GHz) and N_4(9.9112 GHz).

Besides $|3\rangle$-states and $|4\rangle$-states, even higher number states can be produced for certain frequencies, which we show in the table below, on an adjusted time scale (per s, per hr, etc.). On an hourly basis, it is anticipated to have $|5\rangle$-states

Table 2. Estimates of the rates of $|5\rangle$-state, $|6\rangle$-state, $|7\rangle$-state, and $|8\rangle$-state in the radio and microwave range. If any rate is too low, we leave it blank.

ν_0 (GHz)	$N_5(\nu_0)$	$N_6(\nu_0)$	$N_7(\nu_0)$	$N_8(\nu_0)$
0.117	12 per hr			
0.232	11 per hr			
1.078				
1.2378	12 per hr			
1.3711				
2.9334	2 per hr			
3.245	1 per hr			
9.9112	199 per s	3 per s	260 per hr	4 per hr

for some of the frequencies, and for 9.9112 GHz, up to $|8\rangle$-states are expected.

In Berera et al. (2023), we performed estimates on the rates of $|2\rangle$-states at 530.3 nm, 19.664 nm and 1.5 nm transition lines from the solar corona by picking the lower bound whenever a quantity is given in a range. Although being cautious and conservative, this approach underestimated the rates and we revisit the calculations here with more practical values of quantities and so expect higher rates. For the 530.3 nm line, we can assign a value of 20 CI(coronal index) for the intensity according to the observation data during the solar activity cycles (Rušin et al. 2006), which corresponds to a rate of $|1\rangle$-states of $N_1^{530.3} \sim 2.4 \times 10^{13}$. Also, we choose a value of 1.416×10^4 m^{-3} for the density of Fe XIV at the excited level of 530.3 nm Schmelz et al. (2012); Habbal et al. (2011), which is about 40% higher than the one we used in Ref. Berera et al. (2023). Taking these factors into account, the rate of $|2\rangle$-states per second is computed to be $N_2^{530.3} \sim 2062$, while the rates of $|3\rangle$-states and higher are still negligibly small. Turning to the UV emission line of 19.664 nm, where both the intensity of the line (Young et al. 2008) and the density the excited Fe XII ions can acquire larger values, this leads to a rate of $|2\rangle$-states $N_2^{19.664} \sim 1957$. Despite following practical guidelines, the rate of $|2\rangle$-state for 1.5 nm X ray can not be materially improved. The rates of $|2\rangle$-states of optical and UV lines are listed in the table 2.

Table 3. Estimates of the rates of $|2\rangle$-states in the optical and UV range.

λ_0 (nm)	530.3	19.664	1.5
N_1 per s	2.4×10^{13}	1.56×10^{16}	3.78×10^{10}
N_2 per s	2062	1957	~ 0

3. Decoherence & Discussion

Having shown the rates of production of these N-photon states, one may wonder how likely it is for such states to be received by a detector intact without decoherence. Berera et al. (2023) shows the decoherence of photons in the optical to X-ray range is negligible. Therefore, here we mainly consider the possibility of decohering radio and microwave photons. Since the energy of radio/microwave photons are low, they interact with charged particles in the corona predominantly through Thomson scattering, which has a cross section of $\sigma_{\rm Th} = 6.65\times10^{-29}$ m^2. Employing the electron density n_e in the corona given by Wexler et al. (2019), and Edenhofer et al. (1977) respectively, we arrive to a MFP=$1/(n_e\sigma_{\rm Th})$ around 10^{17} m, which is 6 orders of magnitude longer than the distance between the Earth and the Sun.

Another decoherence process could be the scattering of photons off dust particles. The average dust flux measured by In-Situ Helios Krüger et al. (2019) in heliocentric distance range from 0.3 to 1.0 AU is $(2.6\pm0.3)\times10^{-6}$ m^{-2} s^{-1}, with dust radius of 0.37 μm. The shortest wavelength of the radio-microwave photons in our discussion is 5 orders of magnitude longer than the radius of these dust particles. As a result, the scattering would be well described by classical wave diffraction, altering the phase of the photons collectively and leaving coherence unbroken. Dividing the flux by the measured impact speed $\sim$ 60 km/s leads to a number density of the dust of 4×10^{-11} m^{-3}, which further suggests a MFP of $\sim 10^{24}$ m for the scattering. The long MFP for scattering off the dust means such interactions are not significant.

Faraday rotation may be a potential effect, where there is no direct particle interaction. This effect leads to a polarization rotation of angle β which depends on the wavelength λ, the electron density $n_e(s)$ at point s along the path from the solar surface $R_\odot$ to an observer d, and the component of the magnetic field $B_\parallel(s)$ in the direction of propagation. A magnetic field of size $B_\parallel \sim 100$ μT is an overestimate for the value of the magnetic field for the entire region under consideration (Kooi et al. 2022). Using this value and following the calculation in Ref. Berera et al. (2023) for $\beta(\lambda = 100$ nm), yields the rotation angles for the relevant wavelengths in the radio-microwave range of

$$\beta(\lambda = 100 \text{ cm}) \simeq 10^{-4}, \quad \beta(\lambda = 1 \text{ cm}) \simeq 10^{-8}.$$

The electron density and magnetic field strength in Earth's atmosphere are of similar magnitudes as those in the solar corona, but Earth's much thinner atmosphere leads to even smaller rotation angle. This is a small rotation, and

in addition, Faraday rotation impacts photons in the aggregate. Thus, Faraday rotation results in merely an overall rotation without decoherence effects.

The propagation of photons in the Earth's ionosphere could be subject to interactions because the varying electron density changes electric permittivity. However, the plasma frequency of the ionosphere is about 6 to 60 MHz (Jackson 1998), which is much lower than the frequencies considered here. As such, this would at most cause the electric permittivity to barely deviate from 1 and only slightly refract the low frequency photons. Therefore, the ionosphere does not decohere photons that have frequency much higher than 60 MHz.

Another effect, birefringence, usually splits a wave into different paths, depending on the directions of polarization and propagation. For example, $|2_{\boldsymbol{k},s_1}\rangle$ and $|2_{\boldsymbol{k},s_2}\rangle$ have polarization s_1 and s_2 respectively, and birefringence can split them but has no relative effect on individual components of $|2_{\boldsymbol{k},s_1}\rangle$ and $|2_{\boldsymbol{k},s_2}\rangle$. This means for example it affects the two photons of $|2_{\boldsymbol{k},s_1}\rangle$ in the same manner, because they share the same polarization s_1. Consequently, the occurrence of the birefringence does not imply coherence of the state is broken. Similar to the study of effects from gravity (Berera and Calderón-Figueroa 2022), it only induces a change in fidelity, which is distinguished from the loss of quantum coherence.

4. Measurements

Measuring the quantum nature of a signal in space could be significantly more technically demanding than in a terrestrial lab. Since the interactions affecting photons in the radio-microwave frequency range either have very long MFPs or merely change phase uniformly (E.g., we found negligible ionosphere effects and the small Faraday rotations when including the Earth's atmosphere.), our investigations demonstrate that decoherence mechanisms are ineffective against these photons. Therefore, a proposed test of photon coherence within the radio-microwave band can be Earth-based instead of relying on satellites, hence significantly reducing the difficulty and cost of conducting such experiments. Moreover the impact from the Earth's atmosphere can be further reduced by taking measurements on days without clouds (Deng et al. 2019).

Most of the indistinguishability tests of photons are based on the HOM effect (Hong, Ou, and Mandel 1987), in which two identical single photons enter a beam splitter through different input gates but leave through the same exit terminal. Based on the HOM effect, Deng et al. (2019) and Duan et al. (2020) tested quantum interference in the optical range between single solar photons and photons produced by a quantum dot on the Earth, demonstrating distinct evidence for the quantum nature of light. Within the frequency band of our investigation, HOM experiments for microwave photons ($\sim$ 7.25 GHz) from different sources have also been performed (Lang et al. 2013), which provides the blueprint for future experimental setups.

Conventionally the HOM effect is used to test the identicality of two $|1\rangle$ photon states, which coalesce into a single $|2\rangle$ photon state in the standard HOM apparatus. In contrast, our goal is to demonstrate the existence of $|2\rangle$ photon

states from the outset, requiring a HOM test to be run in the time-reversed direction. In a standard HOM setup for testing 7.25 GHz photons (Lang et al. 2013), the length scale of the apparatus is around 1 mm. Among the observed lines we are investigating, is the frequency 9.91 GHz which is relatively close to the 7.25 GHz. Since HOM tests for 7.25 GHz have been successfully conducted experimentally (Lang et al. 2013), we expect that time-reversed HOM tests will also be feasible for 9.91 GHz. Also the apparatus required for testing these photons is anticipated to be of comparable size (approximately 1 mm).

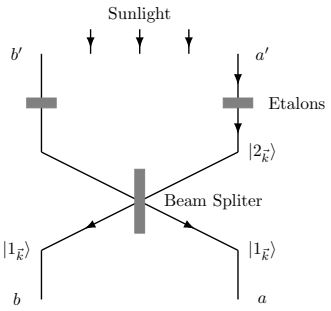


Figure 1. Schematic of a time reversed HOM experiment with two input ports a' and b', etalons, a beam splitter, two output ports a and b connected to further detection and analysis devices. If a $|2\rangle$ photon state enters port a', then it splits into two $|1\rangle$ photon states at the beam spliter, with each $|1\rangle$ photon appearing at ports a and b simultaneously.

A time-reversed HOM apparatus for testing the $|2\rangle$ states consists of two input ports a' and b', two output ports a and b, etalons (Fabry-Perot interferometers) and a beam spliter, as demonstrated in Fig.1. The desired bandwidth of photons can be selectively filtered using etalons, through which only resonant modes will survive. The rate of 9.91 GHz $|2\rangle$ states entering either entrance port, a' or b', is given by $N_2(9.91\text{ GHz}) \times (10^{-3})^2$, or around $2.87 \times 10^1\text{ s}^{-1}$ per HOM device. A $|2\rangle$ state, whether it enters through a' or b', will result in one $|1\rangle$ state exiting from each of the output ports a and b. A time-reversed HOM test favors each photon of the identical $|1\rangle$ pairs simultaneously exiting through each output port, while suppressing the two-photon components $|2\rangle$ at either exit. Note that time reversed HOM tests in a different context have been carried out before (Chen et al. 2018). The identical $|1\rangle$ photon pairs exiting from each of the ports a and b should form a signal, with an average time gap of approximately 34.8 ms between adjacent $|1\rangle$ pairs.

Along with the signal of $|1\rangle$ pairs are a number of $N_1(9.91\text{ GHz}) \times (10^{-3})^2$ background $|1\rangle$ states. These $|1\rangle$ states would enter either a' or b' and exit from either a or b, generating background noise with an average time gap of approximately 0.65 ms between adjacent $|1\rangle$ states.

Even with more total noise than signal, the rates expected here are sufficiently low that the $\sim$ ns resolution of the apparatus is easily able to distinguish between the two, as discussed below. Additionally, polarization distinction between the background and signal photons can help differentiate the two (Chen et al. 2018).

Let us next investigate the ratio of signal to noise for photons received at random as listed in the TABLE 2 in more detail. Again we consider $|1\rangle$ state photons of fixed frequency as noise and $|2\rangle$ state photons of the same frequency as the signal. As above, we will focus on the 9.9 GHz case as an example. The probability of no coincidence P_{nc} in one second in a 1 mm^2 HOM device due to $|1\rangle$ state photons is

$$P_{nc} = \frac{b!}{(b-n)!b^n} ,$$

where b is the number of temporal bin (which we take to be 10^7, i.e., the bins are 100 ns each) and n is the number of 9.9 GHz $|1\rangle$ state photons per second on the device, which is 1540. For b large and $b \gg n$ the approximate probability of a coincidence (i.e., fake signal) is

$$P_c = 1 - e^{\frac{n(n-1)}{2b}} = 11\%.$$

The true resolution of the device is probably closer to 1 ns, which would give $P_c = 0.1\%$. On the other hand, we assume all $|2\rangle$ state photons convert to two $|1\rangle$ state photons, one in each are of the HOM device, so all generate a coincidence. In the 9.9 GHz example that gives a rate of 28 per s in a 1 mm^2 detector. Hence, the experiment is dominated by the signal in this example, and we arrive at the same conclusion for all frequencies listed in the TABLE 2. To summarize, if the inverse HOM effect is efficient, then multi-photon states can easily be detected from the solar corona.

We acknowledge that photons in multiplets created by SE may not have identical momentum due to frequency mismatches, such as Lorentzian or Doppler spectral broadening. However, these broadening effects only reduce, rather than eliminate, the probability of SE. We have also given the rates for high number states including $|3\rangle$, $|4\rangle$ etc. It is worth noting that three-photon interference has been observed (Agne et al. 2017) and there is developing research on the four-photon HOM effect (Ferreri et al. 2019). We also note that other astrophysical quantum experiments in the optical region have been proposed (Dravins 2008; Dravins et al. 2005).

5. Summary

Because of the relations between the production rate of these quantum states and the properties of the solar corona, such as ionic content, thickness and temperature, experimental measurements of the quantum states should unveil new information on the structure of the corona.

Starting from the observational data of solar radio flux and the theory of SE, this work calculated the rates of potentially measurable N-identical photons states $|N\rangle$, originating from the propagation of photons through the stellar atmosphere, specifically, the solar corona. We estimated the rate numbers of detectable $|N\rangle$-states of photons and gave the average expected results in future tests. We demonstrated that various interactions including scattering, Faraday

rotation, etc. are not effective in decohering these quantum states of photons, particularly due to the long MFPs between interactions. We discussed how to measure these quantum states via the time reversed HOM tests, which could be of interest in itself, as it provides a method for distinguishing photons in a $|N\rangle$-state (Bose-Einstein condensates) from those in a $|1\rangle$-state within a collection of photons.

Quantum effects are quite prevalent in the fields of particle physics and condensed matter physics, although they have been slow to emerge in astronomy. This Letter has given an example of how modern techniques developed in quantum optics laboratories can be applied to probe the quantum nature of astronomy. In particular, we have developed a method that uses quantum coherence to provide a valuable alternative probe of the solar atmospheric structure and possibly that of nearby stars. Specifically, measuring the rate of $|N\rangle$ states can reveal the distribution of hydrogen across different energy levels in the solar corona, which is closely tied to the complex temperature profile and density composition of the solar corona. At a fundamental level the measurement of these SE states discussed in this work would be a novel demonstration of quantum coherence of a state sustained over astronomical distance.

Acknowledgements LC is supported by Chizhou University High level Talent Research Start up Fund CZ2025YJRC117. AB is partially funded by STFC. For the purpose of open access, the author has applied a Creative Commons Attribution (CC BY) licence to any Author Accepted Manuscript version arising from this submission.

Author Contribution LC carried out the main calculations of stimulated emission and rate estimations. ZQ contributed to these calculations and performed numerical checks. TK contributed to the development of the theoretical framework and to the calculations of the $|N\rangle$) states. AB made the original theoretical prediction of quantum coherent astrophysical signals and provided theoretical guidance for the present work.

Data Availability All data used in this work are publicly available from the sources cited in the references.

References

Agne, S., Kauten, T., Jin, J., Meyer-Scott, E., Salvail, J.Z., Hamel, D.R., Resch, K.J., Weihs, G., Jennewein, T.: 2017, Observation of Genuine Three-Photon Interference. *Phys. Rev. Lett.* **118**, 153602. DOI. URL.

Aschwanden, M.J., Benz, A.O., Montello, M.L.: 1994, Coherent-Phase or Random-Phase Acceleration of Electron Beams in Solar Flares. *Astrophys. J.* **431**, 432. DOI. ADS.

Aschwanden, M.J., Benz, A.O., Dennis, B.R., Schwartz, R.A.: 1995, Solar Electron Beams Detected in Hard X-Rays and Radio Waves. *Astrophys. J.* **455**, 347. DOI. ADS.

Berera, A.: 2020, Quantum coherence to interstellar distances. *Phys. Rev. D* **102**, 063005. DOI.

Berera, A., Calderón-Figueroa, J.: 2022, Viability of quantum communication across interstellar distances. *Phys. Rev. D* **105**, 123033. DOI.

Berera, A., Brahma, S., Brandenberger, R., Calderón-Figueroa, J., Heavens, A.: 2021, Quantum coherence of photons to cosmological distances. *Phys. Rev. D* **104**, 063519. DOI.

Berera, A., Calderón-Figueroa, J., Chen, L., Kephart, T.W.: 2023, Astrophysically sourced quantum coherent photonic signals. *Phys. Rev. D* **108**, 043033. DOI.

Boyle, L.: 2024, On Interstellar Quantum Communication and the Fermi Paradox.

BROWN, R.H., TWISS, R.Q.: 1956, Correlation between Photons in two Coherent Beams of Light. *Nature* **177**, 27. DOI. URL.

Chen, Y., Ecker, S., Wengerowsky, S., Bulla, L., Joshi, S.K., Steinlechner, F., Ursin, R.: 2018, Polarization Entanglement by Time-Reversed Hong-Ou-Mandel Interference. *Phys. Rev. Lett.* **121**, 200502. DOI. URL.

Deng, Y.-H., et al.: 2019, Quantum interference between light sources separated by 150 million kilometers. *Phys. Rev. Lett.* **123**, 080401. DOI.

Dravins, D.: 2008, Photonic Astronomy and Quantum Optics. In: Phelan, D., Ryan, O., Shearer, A. (eds.) *Astrophysics and Space Science Library*, *Astrophysics and Space Science Library* **351**, 95. DOI. ADS.

Dravins, D., Barbieri, C., Fosbury, R.A.E., Naletto, G., Nilsson, R., Occhipinti, T., Tamburini, F., Uthas, H., Zampieri, L.: 2005, QuantEYE: The Quantum Optics Instrument for OWL.

Duan, Z.-C., Deng, Y.-H., Yu, Y., Chen, S., Qin, J., Wang, H., Ding, X., Peng, L.-C., Schneider, C., Wang, D.-W., Höfling, S., Dowling, J.P., Lu, C.-Y., Pan, J.-W.: 2020, Quantum Beat between Sunlight and Single Photons. *Nano Letters* **20**, 152. PMID: 31841348. DOI. URL.

Edenhofer, P., Lueneburg, E., Esposito, P., Martin, W., Zygielbaum, A., Hansen, R., Hansen, S.: 1977, Time delay occultation data of the Helios spacecraft and preliminary analysis for probing the solar corona. *Journal of Geophysics Zeitschrift Geophysik* **42**, 673.

Ferreri, A., Ansari, V., Silberhorn, C., Sharapova, P.R.: 2019, Temporally multimode four-photon Hong-Ou-Mandel interference. *Phys. Rev. A* **100**, 053829. DOI. URL.

Fontenla, J.M., Avrett, E.H., Loeser, R.: 1990, Energy Balance in the Solar Transition Region. I. Hydrostatic Thermal Models with Ambipolar Diffusion. *Astrophys. J.* **355**, 700. DOI. ADS.

Gabriel, A.H.: 1976, A Discussion on the physics of the solar atmosphere - A magnetic model of the solar transition region. *Philosophical Transactions of the Royal Society of London. Series A, Mathematical and Physical Sciences* **281**, 339. DOI.

Habbal, S.R., Druckmüller, M., Morgan, H., Ding, A., Johnson, J., Druckmüllerová, H., Daw, A., Arndt, M.B., Dietzel, M., Saken, J.: 2011, THERMODYNAMICS OF THE SOLAR CORONA AND EVOLUTION OF THE SOLAR MAGNETIC FIELD AS INFERRED FROM THE TOTAL SOLAR ECLIPSE OBSERVATIONS OF 2010 JULY 11. *The Astrophysical Journal* **734**, 120. DOI. URL.

Hong, C.K., Ou, Z.Y., Mandel, L.: 1987, Measurement of subpicosecond time intervals between two photons by interference. *Phys. Rev. Lett.* **59**, 2044. DOI.

Jackson, J.D.: 1998, *Classical Electrodynamics*, Wiley. ISBN 978-0-471-30932-1.

Kooi, J.E., Wexler, D.B., Jensen, E.A., Kenny, M.N., Nieves-Chinchilla, T., Wilson III, L.B., Wood, B.E., Jian, L.K., Fung, S.F., Pevtsov, A., et al.: 2022, Modern Faraday rotation studies to probe the solar wind. *Frontiers in Astronomy and Space Sciences* **9**, 841866.

Kramida, A., Yu. Ralchenko, Reader, J., and NIST ASD Team: 2023,, NIST Atomic Spectra Database (ver. 5.11), [Online]. Available: `https://physics.nist.gov/asd`. National Institute of Standards and Technology, Gaithersburg, MD..

Krüger, H., Strub, P., Altobelli, N., Sterken, V.J., Srama, R., Grün, E.: 2019, Interstellar dust in the solar system: model versus in situ spacecraft data. *Astronomy & Astrophysics* **626**, A37.

Lang, C., Eichler, C., Steffen, L., Fink, J.M., Woolley, M.J., Blais, A., Wallraff, A.: 2013, Correlations, indistinguishability and entanglement in Hong–Ou–Mandel experiments at microwave frequencies. *Nature Physics* **9**, 345. DOI. URL.

Morgan, H., Cook, A.C.: 2020, The width, density, and outflow of solar coronal streamers. *The Astrophysical Journal* **893**, 57.

Nita, G.M., Gary, D.E., Lee, J.: 2004, Statistical Study of Two Years of Solar Flare Radio Spectra Obtained with the Owens Valley Solar Array. *The Astrophysical Journal* **605**, 528. DOI. URL.

Rušin, V., Minarovjech, M., Saniga, M., Klocok, L.: 2006, Long-term variations of the green coronal (530.3 nm) irradiance. *ILWS WORKSHOP*, 19. URL.

Schmelz, J., Reames, D., Von Steiger, R., Basu, S.: 2012, Composition of the solar corona, solar wind, and solar energetic particles. *The Astrophysical Journal* **755**, 33.

Svelto, O.: 2010, *Principles of Lasers*, Springer.

Townsend, J.S.: 2012, *A modern approach to quantum mechanics*, University Science Books.

Wexler, D.B., Hollweg, J.V., Efimov, A.I., Lukanina, L.A., Coster, A.J., Vierinen, J., Jensen, E.A.: 2019, Spacecraft radio frequency fluctuations in the solar corona: A MESSENGER–HELIOS composite study. *The Astrophysical Journal* **871**, 202.

Young, P.R., Watanabe, T., Hara, H., Mariska, J.T.: 2008, High-precision density measurements in the solar corona. *Astronomy & Astrophysics* **495**, 587. DOI. URL.